Sedimentary Geology 265–266 (2012) 56–71

Contents lists available at SciVerse ScienceDirect

Sedimentary Geology

journal homepage: www.elsevier.com/locate/sedgeo

Holocene evolution of the Great Barrier Reef: Insights from 3D numerical modelling

Samuel J. Barrett [a,b], Jody M. Webster [a,*]

[a] Geocoastal Research Group, School of Geosciences, The University of Sydney, NSW 2006, Australia
[b] Department of Earth Sciences, Royal Holloway University of London, Egham, Surrey, TW20 0EX, UK

ARTICLE INFO

Article history:
Received 16 November 2011
Received in revised form 11 March 2012
Accepted 12 March 2012
Available online 21 March 2012

Editor: B. Jones

Keywords:
Great Barrier Reef
Reef evolution
Numerical modelling
Stratigraphic forward modelling
Reef maturity
Sea level change

ABSTRACT

The Holocene reef in the outer Great Barrier Reef (GBR) represents an archetypal reef system, forming a thin veneer (10–30 m) built upon an older Pleistocene reef surface. The morphology, stratigraphy and maturity (degree of lagoonal sediment infilling) of the modern reef results from the complex interplay between biologic and abiologic processes (reef accretion, sediment erosion, transport and deposition), basement substrate, and Holocene sea level rise. Combining 3D forward stratigraphic modelling (CARBONATE-3D) with a re-analysis of published observational data, we quantitatively simulate the Holocene evolution of One Tree Reef (Southern GBR) as a well constrained, model system, and explore the main processes affecting reef growth in the GBR and elsewhere. We test the influence of different basement substrate surfaces, sea level curves, reef accretion rates, sediment erosion and transport parameters and assess their relative importance in controlling reef evolution—particularly growth histories, 3D internal structure and stratigraphy and reef maturity. Quantitative comparisons between our "best estimate" model output and the observed data confirm that we are able to simulate a 75% match of the main morphologic and growth characteristics of One Tree Reef. The range of parameters tested produced the full spectrum of reef maturities from unfilled "juvenile" buckets to planar "senile" reefs with completely sediment infilled lagoons. We conclude that the shape and depth of the basement substrate has the strongest influence—significantly impacting reef evolution and final maturity including the shape of the "bucket", the size of the reef margins and internal reef structure. In contrast, variations in sea level, sediment production, erosion and transport mainly controlled the degree of lagoonal sediment filling. This study has implications for better understanding the past evolution of the GBR and other reefs but also lays the foundation for improved predictions of possible trajectories of modern reefs in general in the face of future environmental changes.

1. Introduction

The modern Great Barrier Reef (GBR) forms a relatively thin Holocene veneer (10–30 m (Hopley et al., 2007)) overlying an older Pleistocene reef substrate (Marshall and Davies, 1984). The evolution of the Holocene reef is influenced by the complex relationship between this initial basement substrate, sea level change, oceanography (e.g., wave energy and direction), biological accretion (e.g., coral growth patterns) and abiologic sedimentation (e.g., Davies and Montaggioni, 1985; Davies et al., 1988; Hopley et al., 2007; Montaggioni and Braithwaite, 2009). Based on over 20 years of shallow drilling (see Hopley et al., 2007 for a summary) considerable progress has been made towards understanding the general pattern of Holocene reef evolution. Investigation of cores from One Tree Reef in the southern GBR (Fig. 1), allowed Marshall and Davies (1982) to propose the prevailing model of Holocene reef development, with initially vertical growth in response to rising sea level, followed by mainly leeward directed growth after reaching present sea level. Despite these conceptual advances there is still considerable uncertainty about relationships between these factors and their influence on reef morphology, stratigraphy, accretion and biosedimentological composition (herein termed architecture), particularly with respect to their 3D spatial variability. To date our understanding of the temporal and spatial patterns of the Holocene development of the GBR and elsewhere comes mainly from 2D conceptual cross sections derived from relatively sparsely-spaced drill core data (Hopley et al. 2007; Montaggioni and Braithwaite, 2009).

In addition to the general model of reef development proposed by Marshall and Davies (1982), several workers (Hopley, 1982; Hopley et al., 2007; Davies, 2011; Hopley, 2011) have proposed a genetic classification system for Holocene reefs based on the stage of rim development and lagoonal filling (see also Davies 1983 with examples and a slightly modified system). These stages are categorised as "juvenile", "mature" or "senile"/planar (with sub-categories) ranging from patchy reef accretion on antecedent topographic highs (juvenile) to lagoonal reefs (mature—e.g., One Tree Reef and Fitzroy Reef) to flat-topped, sediment filled reefs (senile/planar—e.g., Wreck and Fairfax Reef) (Fig. 1). These stages of reef maturity are distributed

* Corresponding author. Tel.: +61 2 9036 6538; fax: +61 2 9351 0184.
E-mail address: jody.webster@sydney.edu.au (J.M. Webster).

0037-0738/$ – see front matter © 2012 Elsevier B.V. All rights reserved.
doi:10.1016/j.sedgeo.2012.03.015

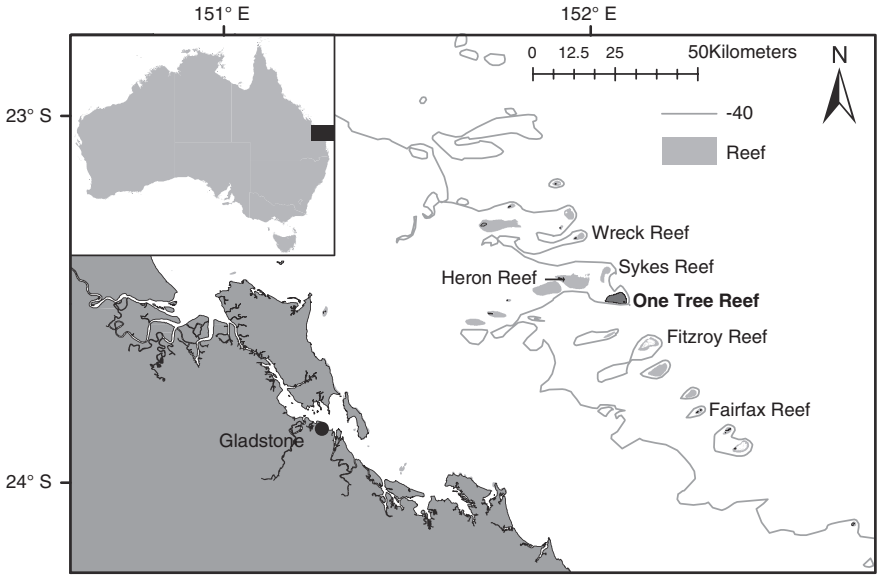

Fig. 1. Location map showing One Tree Reef, southern Great Barrier Reef.

across the GBR (see Hopley et al., 2007) and much of the sequence except for the earliest juvenile stages is represented in the same small geographic areas (e.g., 70 km in the Capricorn-Bunker group) indicating that local rather than regional factors must explain the variation. The full range of controls on reef maturity are not known, but factors such as reef size, depth to the antecedent surface and carbonate production are considered key. However, observational data to test these hypotheses are sparse with Davies (1983) and Hopley et al. (2007) also suggesting that to better understand how reefs evolve and mature, we must move beyond simply descriptive observations and quantitatively investigate the processes that control reef development.

Forward Stratigraphic Modeling (FSM) has been used successfully to predict the structure and stratigraphy of carbonate platforms on a range of spatial and temporal scales (e.g., Warrlich et al., 2002; 2008). The interactions between known processes can be explored and sensitivity testing used to assess their relative importance in controlling the 3D structure and stratigraphy of sediment bodies. Weaknesses and limitations in models may also shed light on important but previously unknown or poorly constrained processes. In this paper we use the SFM software CARBONATE 3D (CARB3D) (e.g., Warrlich et al. (2002)) to investigate the main processes that have controlled the Holocene evolution of the GBR, particularly the 3D internal structure, sedimentary facies distributions and overall reef maturity concepts. One Tree Reef provides a unique real-world laboratory to address these questions given the wealth of observational data characterizing the modern physical processes (e.g., Frith and Mason, 1986 and Harris et al., 2011), surface zonation (Davies et al., 1976), and development of the Holocene reef based on the most comprehensive suite of Holocene reef cores (Marshall and Davies, 1982) available for the GBR.

Here we present a synthesis of 3D numerical modelling results, groundtruthed against real-world observations from One Tree Reef. Our objectives are to: (1) accurately simulate the Holocene evolution of the reef over the last 9 ka; (2) investigate the relative importance of the main factors (basement substrate, sea level rise, accretion rates, erosion and sediment transport) that influence reef morphology (and maturity); (3) investigate the impact of these factors on the 3D architecture of the reefs, and finally; (4) discuss the implications of this model-observational data approach for predicting possible coral reef trajectories in response to future environmental changes.

2. Study site and methodology

2.1. One Tree Reef—modern setting, internal structure, and Holocene evolution

One Tree Reef, part of the Capricorn-Bunker group, is 5.5 km by 3 km (Fig. 1). A small coral-shingle cay occurs on the windward margin called One Tree Island with raised windward and leeward margins surrounding a lagoon bordered by sub-tidal sand sheets on its southern and eastern sides (Fig. 2A) (Davies, 1983). Marshall and Davies (1982) described the morphology, zonation and internal structure of One Tree Reef using surface observations and drill core data (Fig. 2B, C). They defined five biological/sedimentological surface and subsurface facies: algal pavement, coral head facies, branching coral facies, reef flat rubble facies and sand facies which can be further grouped into mainly in situ growth (i.e., algal pavement, coral head and branching coral facies) and re-deposited material (i.e., rubble and sand facies).

Holocene reef growth at One Tree (Marshall and Davies, 1982, Davies et al., 1989) initiated about 8 ka, after sea level flooded the palaeo-high formed by the Pleistocene reef. Reef growth lagged behind sea level rise until sea level stabilised about 6.5 ka when the reef began to catch-up. The windward margin caught up with sea level about 5.5 ka with the leeward margin catching up around 1 ka later. The coral head and branching coral facies that characterised the vertical growth phase were replaced by algal pavement and rubble flat facies given the lack of accommodation space (and increasing energy). Lateral and leeward progradation has dominated since from both margins with the central lagoon continuing to infill with sand (Fig. 2A and Supp. Table 1 for calibrated ages).

2.2. Numerical model parameters and justification

CARB3D is a sophisticated FSM tool incorporating various modes of carbonate production along with sediment erosion, transport and deposition, coupled with complex sea level changes and initial surfaces (Warrlich et al., 2002). The software has been used to simulate carbonate systems on a wide range of spatial and temporal scales (Warrlich et al., 2008). CARB3D calculates and displays "process-based facies" production including platform margin, platform interior, and re-deposited sand (Warrlich et al., 2002). However, "defined facies" based on the proportion of platform margin (i.e. coralgal

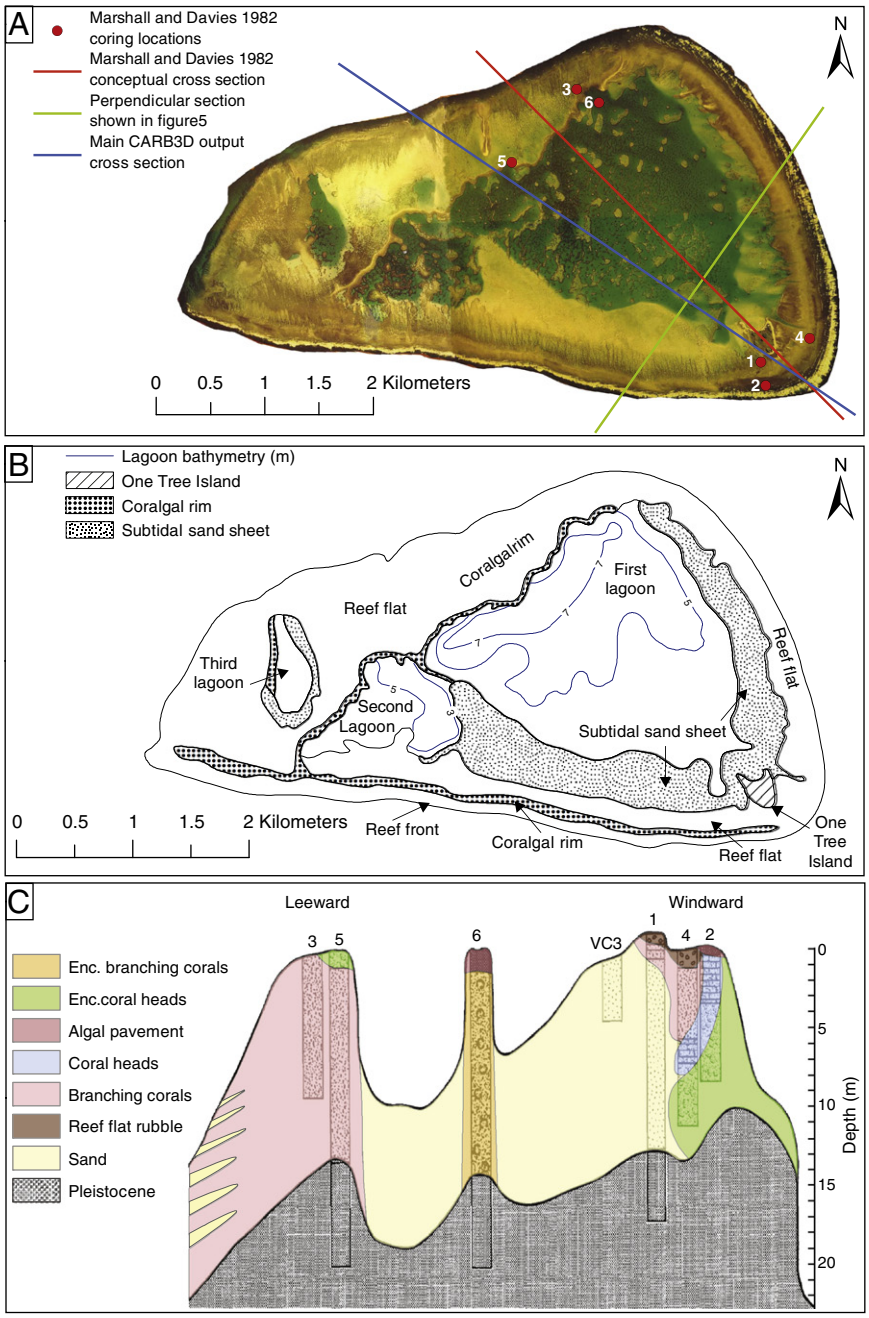

Fig. 2. A: Aerial image of One Tree Reef showing previous drill cores, observational and numerical cross sections referred to in this study. B: Reef zonation map re-drawn after Davies et al. (1976). C: Cross section showing Holocene reef cores, the Pleistocene substrate and the conceptual distribution of the main sedimentary facies (re-drawn after Marshall and Davies (1982)) (Enc. = encrusting).

framework) material, sand and fine grained material can also be simulated within a grid cell using a modified Dunham classification scheme (Dunham, 1962 and Embry and Klovan, 1971) (Fig. 4B). The most important model parameters are summarized in Table 1 and their scientific justification discussed below with respect to available field observations.

2.2.1. Initial surface/basement substrate

Based on extensive drilling and seismic refraction data (Davies et al., 1977, Harvey et al., 1979, Marshall and Davies, 1982, Marshall and Davies, 1984) we constructed a new 3D model of the initial Pleistocene surface at One Tree Reef, including surrounding shelf, on which the Holocene reef grew (see Supp. Table 2 and Video 1 for data). Drill core data through the windward margin show the surface at 13 m below current mean sea level (mbsl) while on the leeward margin it is between 15 and 17 mbsl (Marshall and Davies, 1984). The seismic refraction data show large variations (10–23 mbsl) in the surface indicating a highly irregular karst topography locally (Harvey et al., 1979; Harvey and Hopley, 1981). Unfortunately, the seismic refraction data are too sparse so some assumptions are needed to estimate the locations and widths of the rims of the Pleistocene surface. To create our initial surface, the windward and leeward rims of the Pleistocene surface were assumed to be similar in width and location to the modern rims (Davies et al., 1989) with the modern gradient used from the palaeo-rim tops to the shelf floor. For the lagoon, one core penetrates a patch reef into the Pleistocene at 14 mbsl (Fig. 2) but this may be on palaeo-high and not representative of the general Pleistocene surface beneath the lagoon (Marshall and

Table 1
Summary of significant input parameters and testing values with "best estimate" values in bold.

Carbonate 3D model input parameter	Value	Units	Justification
Run time	13.65	ka	Time from flooding of lowest point on initial surface to the present day
Time step	0.1	ka	Compromise between resolution and model run
Cell size	100×100	m	Time (approx. 5 min per test)
Area of simulation	13×9	km	Modern One Tree Reef extent plus buffer
Maximum platform margin production rate	4, 10, 12, **14**, 16, 20	m/ka	Close to maximum measured in Indo-Pacific
Top depth of maximum PM rate interval	0	m	Sea level
Bottom depth of maximum PM rate interval	5	m	Carbonate production-depth studies in Indo-Pacific
Scale depth for platform margin production	8	m	As above
Platform interior production rate	0.7	m/ka	Lagoon accretion rate measured at One Tree Reef
Horizontal restriction scale	1750	m	Size of observed modern lagoon
Maximum disintegration rate	0, 0.025, 0.05, **0.06**, 0.07, 0.1, 0.14	m/ka	Caribbean measured erosion rates
Lowest depth of maximum disintegration	2	m	Apparent depth of destructive surf zone from core data
Scale depth for disintegration rate	2.5	m	As above
Maximum shear stress	0, 0.5, 1, **2**, 2.5, 3, 5	N/m^2	Order of magnitude estimate
Shear stress direction	320°	bearing	Modern swell and wind directions

Davies, 1982). Seismic refraction data suggests its depth varies between 16 and 23 mbsl (Davies, 1977; Harvey et al., 1979).

Taken together, our "best estimate" of the initial Pleistocene surface is: 13 mbsl beneath the windward margin, 17 m below the leeward margin and 22 m below the present day lagoon (Fig. 4A). While not identical, this is consistent with the shape of the Pleistocene surface at the adjacent Heron Reef and a general 'bucket' shape morphology (Hopley et al., 2007), much like the modern day reefs, with a central depression (lagoon) surrounded by raised rims. However, to test the effect of different initial surface depths and morphologies on Holocene reef evolution, we created and tested several basement substrate types (Fig. 6A–D). The differences between these surfaces represent changes to the depth of the lagoon (if present) or the height of the flat-topped platform (if no lagoon is present).

2.2.2. Sea level change

In our numerical model, we use estimates of relative sea level change over the Last Glacial cycle based on fossil reef sequences at the Huon Peninsula (Papua New Guinea) and sediments from the Bonaparte Gulf (NW Australia) (Lambeck and Chappell, 2001). We used the midpoint between the upper and lower bounds of this curve in our model runs which ran between 13.65 and 0 ka, and started at 65 mbsl, the deepest point on our initial surface. The data were smoothed to avoid any unrealistic kinks or sea level reversals (Hopley et al. 2007) caused by our method of picking the midpoint combined with uncertainties of actual sea level data. The curve used in the best estimate simulations is shown in Fig. 4C and reaches present sea level ~6.5 ka. Subsidence is not considered because over the model run period subsidence is small (20–30 cm) (Davies, 1983) and well within the error bounds of the sea level curve. To test the effect of different sea level curves on reef evolution, the final period of the sea level rise from the point of flooding of the shallowest part of the initial surface was varied. For example, Fig. 8 shows variations in the timing of when the sea level rise reached present level: at 3 ka and at 0 ka simulating a Caribbean style sea level rise (Toscano et al., 2011) (instantaneous flooding was also tested). Very rapid rises, similar in rate (25–45 m/ka) to those associated with melt water pulses observed in the last deglaciation 14–15 ka (i.e., MWP-1A) were also tested (Fairbanks, 1989; Bard et al., 1990). Finally, to investigate the effect of less accommodation space we tested curves offsets vertically by −2 m and −5 m from the best estimate.

2.2.3. Reef accretion rates (platform margin production)

Available drill core data provide important constraints on the vertical accretion rates for a range of reefal facies in the GBR. Rates up to 16 m/ka for branching coral facies, and 7 m/ka for coral head facies, are reported (Davies and Hopley, 1983). The maximum vertical accretion rate measured at One Tree Reef is 8.3 m/ka in coral head facies (Marshall and Davies, 1982), broadly similar to rates across the Indo-Pacific summarised by Montaggioni (2005). In CARB3D, 'Platform Margin Production' is directly analogous to coralgal framework accretion (Warrlich et al., 2008) which, in the case of One Tree Reef, dominates the windward and leeward reef rims and slope. The rate of production in the model is initially calculated for each cell in respect to depth. This production value is then restricted by a range of factors including platform interior restriction (e.g., lagoonal restriction of coral growth due to increased salinity), sediment flux restriction and erosion. The initial depth controlled vertical accretion is specified by a maximum accretion rate, the interval over which this rate is constant, and a scale factor controlling the shape of an exponential curve defining the rate below the bottom depth for the maximum rate (Warrlich et al., 2002; Webster et al., 2007).

Warrlich et al. (2002) determined the depth profile of carbonate production from modern carbonate production studies. A synthesis of vertical accretion versus depth data from the GBR (Hopley et al., 2007 and Hopley, 2011) suggest accretion is attenuated with depth due to restriction and erosion. However, carbonate production data (mass rather than vertical accretion) (Hubbard et al., 1990; Vecsei, 2001) suggest production is highest in the upper few meters of the water column and reduces exponentially with depth. As CARB3D models the effects of restriction and erosion, the initial simulated carbonate production-depth profile should mirror the observed carbonate mass production studies. Further, the final modelled vertical accretion rates should reflect the pattern of the vertical accretion versus depth studies. The exact relationship between carbonate production mass and vertical accretion is unclear (Davies and Hopley, 1983) and the units of measurement are different. Therefore, the most appropriate interval of maximum production and exponential scale factor below this value, was determined by fitting a curve to the shape of the Indo-Pacific carbonate production values (Vecsei, 2001) (Fig. 3). In this way a maximum production interval of between 0 and 5 m with an exponential scale factor of 8 m was established.

In the model the maximum potential vertical reef accretion is only possible under perfect conditions, before the effects of restriction and/or erosion are taken into account. As the different restricting factors overlap (e.g., maximum production occurs in the erosion zone) this maximum can never be obtained in the model and will rarely, if ever be represented in reality. Therefore the maximum rate will be similar to the highest observed vertical reef accretion rates and may be slightly higher, than the ideal value derived from sensitivity testing of the model itself. Using available observational data, 14 m/ka was chosen for the best estimate value while 10 m/ka, 20 m/ka and a lower value of 4 m/ka observed at One Tree Reef by Marshall and Davies (1982), were used for sensitivity testing (Table 1).

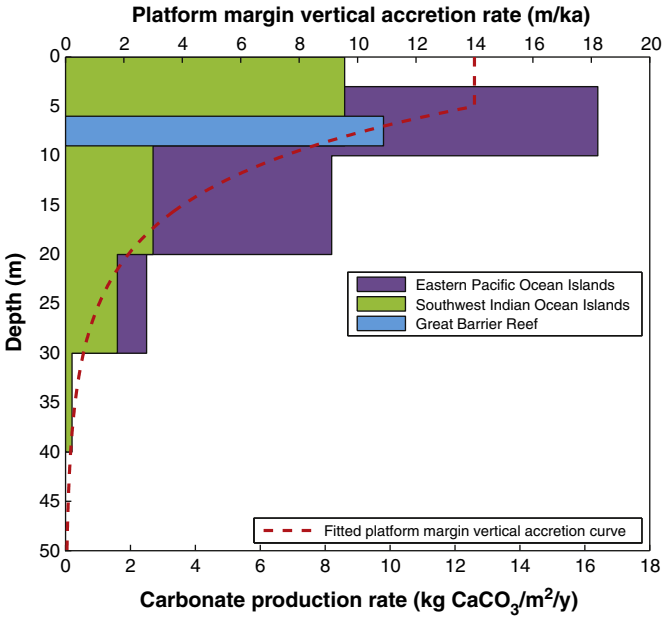

Fig. 3. Relationship between platform margin production and depth. Carbonate production from the Indo-Pacific region was estimated using a census based method (modified from Vecsei, 2001) and fitted against the maximum platform margin vertical accretion curve. The parameters which define the shape fitted curve are: bottom interval of maximum production—5 m depth, exponential scale factor—8 m and maximum production rate—14 m/ka.

2.2.4. Lagoon/platform interior production

Lagoonal sediment at One Tree Reef is mainly comprised of sand with significant mud and gravel locally (Davies et al., 1976; Frith and Mason, 1986; Hopley et al., 2007; Davies, 2011). In the model, we therefore define two categories of lagoonal sediment based on their texture and source. The first are coarse grained sediments generated by the disintegration and transport of coralgal framework from the reef rim (Davies, 1983) and the second are a mud component derived from disintegration of in situ *Halimeda*, bivalve shells and benthic foraminifera tests (Montaggioni and Braithwaite, 2009). Overall lagoonal accretion rates range from 0.5 to 1.7 m/ka for One Tree Reef (Davies, 1983) and 0.7 to 2.1 m/ka for nearby Heron Reef (Smith et al., 1998).

In our simulations 'Platform Interior Production' is analogous to in situ production of fine grained sediment in the lagoon and on the adjacent shelf. Coarse grained sedimentation is simulated by disintegration and transport of platform margin production (coralgal framework) so the parameters here refer only to in situ production of fine grained sediments. We assume the upper bounds of the observed lagoonal accretion rates include a substantial proportion of transported coarse grained sediments and the lower bound represent mainly in situ production and therefore a maximum rate of 0.7 m/ka is used for the best estimate. To establish how platform interior and margin production rates vary by location, restriction is calculated using both horizontal and depth scale factors. Warrlich et al. (2002; 2008) recommend using a horizontal scale value similar to the size of the expected or present day lagoon. The One Tree Reef lagoon is comprised of three separate lagoonal areas, but the largest has a diameter between 1.2 and 2.2 km (Fig. 2A) so a value of 1.7 km was used.

2.2.5. Disintegration–sediment generation

Disintegration rates of coralgal boundstones depend on the substrate properties and their relationship with various biological, chemical and physical processes operating in different reef environments (Montaggioni and Braithwaite, 2009). Davies (1983) reported values varying by two orders of magnitude in the Indo-Pacific region while Trudgill (1983) observed rates for One Tree between 0.2 and 2.9 m/ka. In the Caribbean, Spencer (1985) calculated rates between 0.1 and 3.6 m/ka depending on reef setting and lithology. Holocene GBR drill cores commonly record reduced vertical accretion rates within 2–3 m of sea level confirming the importance of erosion in the surf zone (Davies and Hopley, 1983).

CARB3D simulates erosion by the disintegration of substrates and subsequent transport of sediment due to shear stress. Like platform margin production, a maximum disintegration value, the interval of this value and an exponential scale factor below this interval are defined. However, the published data indicate erosion rates are highly variable locally, so the use of single erosion rate regionally, regardless of local variation, presents a challenge. We performed initial simulation experiments using reported values and found a disintegration rate of 0.06 m/ka produced realistic behaviour and was used in the best estimate scenario. We chose values between 0 and 0.14 m/ka for sensitivity testing and a depth interval of 0 to 2 m for the maximum disintegration wave zone, with below 2 m defined by an exponential scale factor of 2 m.

2.2.6. Sediment transport and deposition (shear stress)

Disintegration only becomes erosion when the disintegrated sediment is transported. Patterns of sediment transport and deposition at One Tree Reef are controlled by wind induced waves and tidal currents (Davies et al., 1976). The dominant wind and swell direction is from the south east, however, locally, wave refraction controls the dominant energy and water flow direction (Davies, 1977). Modeled velocities in the lagoon fluctuate significantly spatially and temporally during the tidal cycle and with changing wind conditions (Frith and Mason, 1986). Direct observations from One Tree Reef and other nearby reefs show flow velocities of between 5 and 80 cm/s with an average of about 25 cm/s (Davies and Kinesy, 1977 and Harris et al., 2011).

CARB3D uses shear stress and slope to determine the entrainment and deposition of sediment (Warrlich et al., 2002). Shear stress is related to the water flow velocity directly above the substrate. However, the role and magnitude of shear stress in carbonate sediment transport is still poorly understood (e.g., Kench and Brander, 2006). CARB3D allows only one constant shear stress magnitude and direction across the model which does not account for the high spatial and temporal variability possible in the real world (e.g., rubble transport and deposition).

The modelled and observed variations in flow velocity and the lack of a more complex hydrodynamic model required initial experimental testing to find an appropriate value. A value of 2 N/m^2 from the south east showed behaviour consistent with observed data and model expectations and values between 0 N/m^2 and 5 N/m^2 were used for sensitivity testing. Similar values were used in previous applications of CARB3D (Warrlich et al., 2008) and they are also consistent with the modelled shear stresses from a range of modern reef environments (Storlazzi et al., 2011).

2.3. Geomorphic observational data

Several bathymetric data sets were used to build the initial surface but also to provide geomorphic constraints with which to test the model outputs. Regional bathymetry was provided by a 250 m grid (Webster and Petkovic, 2005) and local bathymetry for One Tree and adjacent shelf provided by a 25 m grid from a Laser Airborne Depth Sounder (LADS) survey (Australian Hydrographic Service). Observations from Frith and Mason (1986) provided additional constraints on bathymetry of the lagoon. These datasets were mosaiced together in ArcGIS to form a continuous bathymetry data set for study area, and combined with aerial imagery, were used to test model outputs against actual modern reef morphology. Table 2 summarizes the key 'morphometrics' and how they were calculated, as

Table 2
Observational "morphometrics" used to test model outputs.

Morphometric		Value	Source
Lagoon	Area	~5.8 million m^2	Calculated from LADS data and aerial photographs
	Volume	~19.4 million m^3	Calculated from bathymetry from Frith and Mason (1986)
	Maximum depth	~>7 m or ~>6 m	Davies et al. (1976) or Frith and Mason (1986)
	Average depth	3.2 m	Calculated from bathymetry from Frith and Mason (1986)
Sea level	Windward	~4.2/5.6 ka	Marshall and Davies (1982)
Catch-up time	Leeward	~4.5 ka	Marshall and Davies (1982)
Reef vertical accretion rates	Windward—coral head facies	1.8–7.3 m/ka	Marshall and Davies (1982)
	Leeward—branching coral facies	0.6–8.3 m/ka	Marshall and Davies (1982)
Reef flat/rim width	Minimum	~120 m	Aerial photographs
	Mean	616 m	Aerial photographs
	Median	593 m	Aerial photographs
	Maximum	~1212 m	Aerial photographs

well as other important observational data (i.e., timing of sea level catch-up).

3. Results and basic interpretations

Initial model testing with realistic parameters based on the observational data (Table 2) and known model behaviour, allowed us to produce a "best estimate" set of parameters (Table 1) and model output (Fig. 4). To establish the impact of each parameter on reef evolution (including reef maturity), numerous sensitivity experiments were also performed changing one parameter at a time while keeping the others constant. The results of these experiments, along with the best estimate output, are compared with the observed data and summarized below.

3.1. Best estimate model outputs

A cross section (see Fig. 2A for location) through the 3D best estimate model shows the internal process-based and defined facies patterns through the simulated reef (Fig. 4 and Supp. Video 1). A 3D section through the model output (Fig. 5) also confirms the internal complexity and spatial heterogeneity of the CARB3D simulation. The windward and leeward rims are both dominated by platform margin (i.e., coralgal framework) material with the lagoon being dominated by re-deposited sand with minor fine grained platform interior and platform margin components (i.e., varying proportions of sand, mud and framework) (Fig. 4A, B). Morphologically and stratigraphically, the model output is broadly consistent with the observed surface and subsurface reef data (i.e. conceptual cross section in Fig. 2C vs.

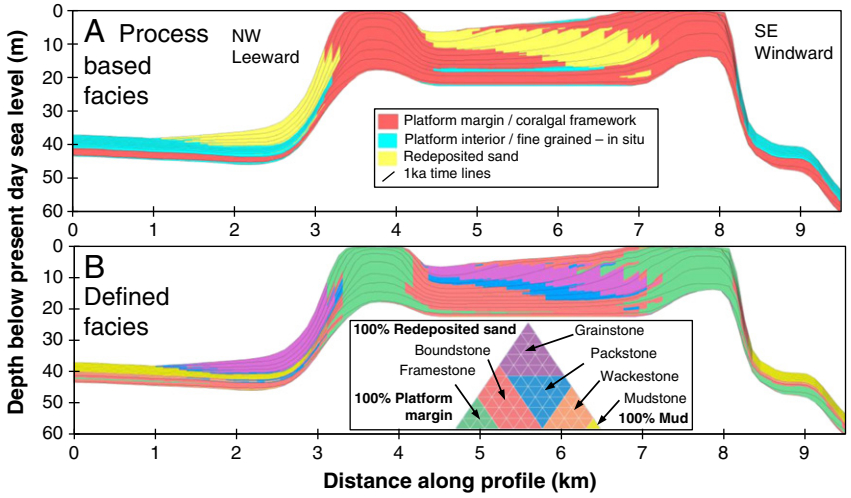

D

		Best estimate	Actual	Best estimate / Actual %
	Lagoonal area (km^2)	7.26	5.84	124%
	Mean lagoon depth (m)	2.85	3.32	86%
	Unfilled lagoon volume (million m^3)	20.72	19.42	107%
Windward	Sea level catchup (ka)	3.7	4.2-5.6	66-88%
	Maximum vertical accretion (m/ka)	5.15	-	-
Leeward	Sea level catchup (ka)	2	~4.5	44%
	Maximum vertical accretion (m/ka)	3.86	-	-
Lagoon	Maximum vertical accretion (m/ka)	4.27	-	-

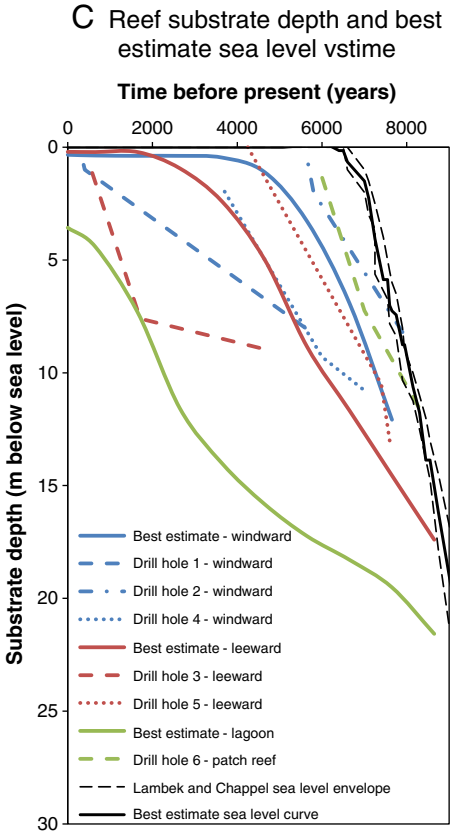

Fig. 4. Best estimate model output. A: Cross section through the 3D model showing process-based sedimentary facies (see Fig. 2A for profile location). B: Cross section showing defined facies (ternary plot). C: Best estimate sea level curve and modelled reef growth curves for the lagoon, windward and leeward margins (solid) compared to observed growth curves from age data from the One Tree Reef drill cores (dashed and dotted). D: Model output metrics compared to the observational data (lagoonal area, depth and volume), vertical accretion rates and calculated sea level catch-up time (summary in Table 2). All radiocarbon dates were converted to calibrated ages (ka) using CALIB 4.4 (MARINE.98 calibration data set after Stuiver et al., 1988).

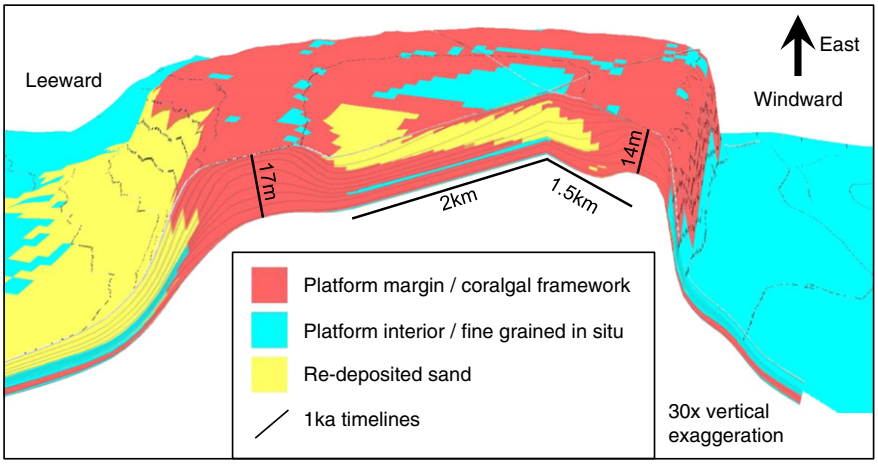

Fig. 5. 3D visualization looking east through the best estimate model output.

Fig. 4A and surface morphology Fig. 2A, B vs. Fig. 5). For example, the modelled lagoon is broadly similar in size, shape and depth to the observed lagoon and also deepens leewards (Fig. 4D). However, the modelled margins are wider than the observed (Fig. 2A), nor does the model simulates the prominent sand aprons currently observed behind the reef flat (Fig. 2A).

Modelled reef accretion curves show how the reef accreted towards sea level in windward and leeward margin and lagoon. The timing of sea level catch-up in the models was defined as the time at which the reef surface was within 0.5 m of present sea level. Comparison with the observed data (Marshall and Davies, 1982; dashed and dotted lines Fig. 4C) reveals that the general shape of the modelled accretion curves are consistent but the timing of when parts of the reef reached sea level is significantly later. The modelled accretion rates are within the range of observed rates, with a maximum vertical accretion of 5.2 m/ka at the windward margin in the model, slightly lower than the observed maximum of 8.3 m/ka.

The similarity between the best estimate model output and the observed reef morphology and structure shows that it is necessary and valid to use platform margin production model inputs significantly greater than observed coralgal vertical accretion rates (14 m/ka vs. 8.3 m/ka observed at OTR (Marshall and Davies, 1982)). These high rates allow the observed rates to be realised in the model after the effects of erosion and restriction of coralgal growth. Testing also shows that beyond a threshold level (15 m/ka), there is little difference between the model outputs for both morphology and catch-up time. This suggests that other limiting factors become more important in controlling reef growth beyond this level. It is these limiting factors which may act to restrict the overall modelled growth rate in all model scenarios so that the modelled time of reef catch-up to sea level is never as early as in real life.

3.2. Initial surface tests

Sensitivity testing confirmed that shape and depth of the initial surface has profound impacts on the model outputs (Fig. 6). This is consistent with previous seismic investigations from the Capricorn Group that concluded that the modern day reef morphology was largely determined by the shape and depth of the Pleistocene basement substrate (Searle et al., 1982; Harvey et al., 1979; Marshall and Davies, 1982). In particular, we find that the depth of the initial central lagoon has a significant impact on the morphology, internal structure and composition of the final output. The common pattern of raised rims with a deeper lagoon in the centre, the so called "bucket" morphology, is present in all of the initial surface outputs to some extent although the comparative depth of the bucket and the level of infilling varies. For example, scenarios (Fig. 6C, D) with flat tops with no initial depressions can form raised rims with some sort of lagoonal area although the "bucket" morphology is less pronounced. This shows that the "bucket" morphology is not dependent entirely on the initial surface but could result from differential reef accretion of Holocene reefs (Purdy and Gischler, 2005; Schlager, 2005). However, Holocene growth in CARB3D does appear to amplify any features (e.g., raised rims Stoddart, 1973, Hopley et al., 2007) from the initial surface resulting in a deeper bucket than was present initially (e.g., Fig. 6B).

The initial surface also has a significant impact on the amount of leeward progradation. Scenarios with deeper lagoons have smaller sand wedges whereas those with a flat top generally have larger ones (Fig. 6A, C vs. B and Fig. 4A). With a lagoon, material eroded from the windward margin is collected in the lagoon and the leeward sand wedge is comprised of material eroded from the leeward margin only. In situations with no lagoon to act as a sediment sink to the windward sediment production, this sediment is added in whole or in part to the leeward wedge increasing its size (Davies, 1983).

The highest modelled vertical accretion rates are at the windward margin with the highest realised in the best estimate scenario with a shallow initial bucket shape (Fig. 6E). Lagoon maximum accretion rates are higher than leeward maximums in examples with raised rims (e.g., Fig. 6A and B) but are lower than the leeward maximums in flat-topped examples. The windward margin reaches sea level before the leeward margin in all scenarios with initial raised rims. However, the leeward margin reaches sea level earlier than the windward margin in the 10 m and 13 m flat top scenarios. This finding is inconsistent with the observed cross section and could be caused by the model "pausing" at the windward margin just below the 0.5 m sea level catch-up "threshold". An analysis of the relationship between the total accommodation space (volume of space between initial surface and current sea level with no Holocene accretion) and the modelled unfilled lagoon volume and depth confirm the positive correlation between accommodation space and both final unfilled lagoonal volume and depth.

3.3. Platform margin production rate tests

The maximum platform production rate has a significant effect on the reef morphology and facies distributions (Fig. 7). With a rate of 4 m/ka, the reef is unable to reach sea level and the final morphology closely mimics the initial surface/basement substrate (Fig. 7A). In contrast, a rate of 20 m/ka produces only a small and shallow lagoon with platform margin facies dominating (Fig. 7D), but interestingly, does not completely infill the lagoon. It appears that restriction

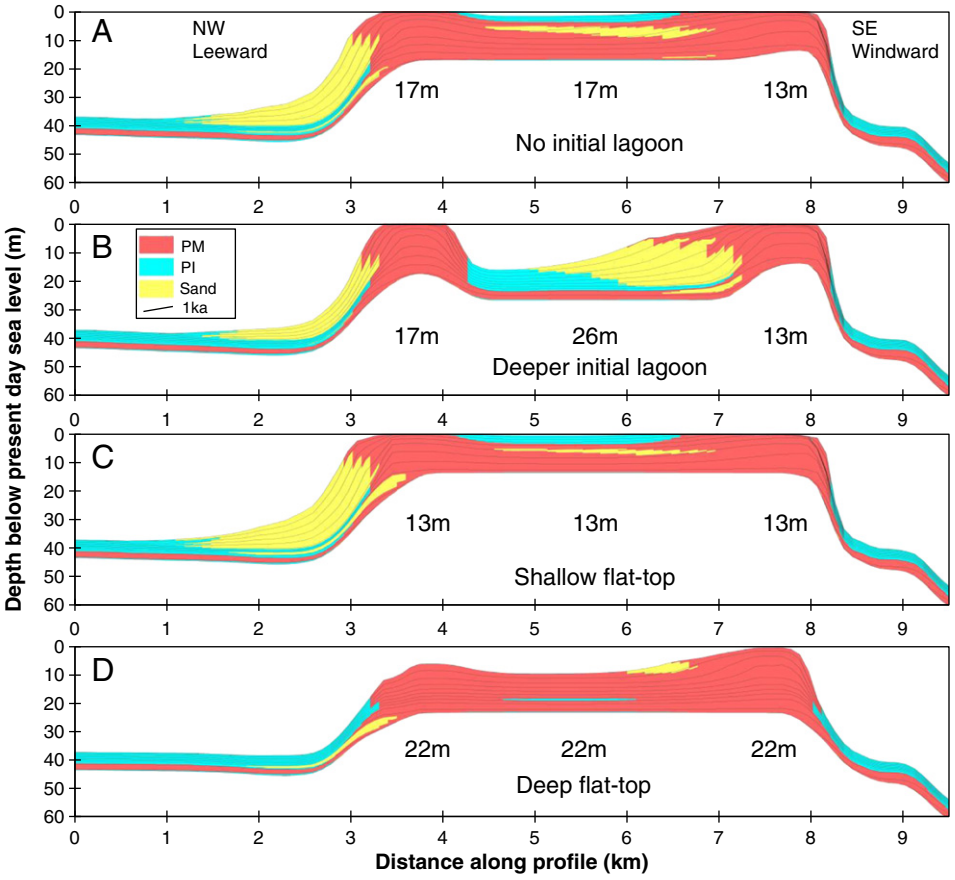

E

	Windward, leeward, lagoonal depth	13,17,17	13,17,22 (Best estimate)	13,17,26	10,10,10	13,13,13	17,17,17	22,22,22
Windward	Sea level catch-up (ka)	3.7	3.71	3.81	1.48	2.75	1.67	-
	Max. vertical accretion (m/ka)	4.88	5.15	5.11	4.61	5.09	4.36	3.80
Leeward	Sea level catch-up (ka)	1.81	2.04	2.80	3.97	3.60	-	-
	Max. vertical accretion (m/ka)	3.59	3.86	3.99	3.32	3.54	3.24	2.77
Lagoon	Max. vertical accretion (m/ka)	3.83	4.27	2.72	2.56	3.22	2.94	2.02

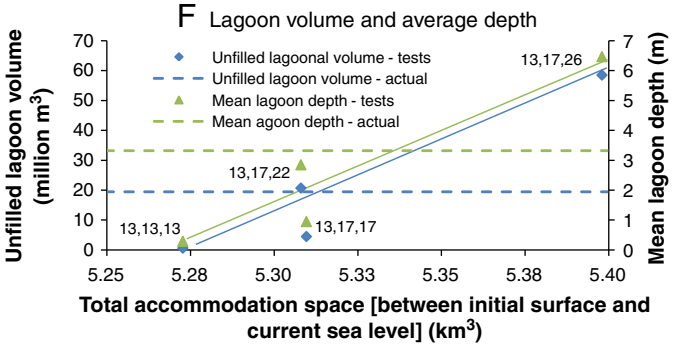

Fig. 6. Initial surface/basement substrate model output test. A–D: Cross sections showing process-based sedimentary facies for different initial surface scenarios. E: Table showing rates and time of sea level catch-up for each scenario. F: Plot showing the relationship between model lagoon depth and volume and the available accommodation space above the initial surface. Key: PM—Platform margin/coralgal framework, PI—Platform interior/fine grained in situ.

prevents increased platform margin accretion in the centre of the reef. However, testing of high production rates (25 m/ka) combined with very high disintegration (erosion) rates (0.14 m/ka) did result in complete and rapid infilling of the lagoon with re-deposited sand and significant leeward sand wedge progradation. Both the lagoonal area and depth are affected by changing rates with higher rates resulting in wider rims and a greater proportion of lagoonal infilling, and therefore, a smaller lagoon. Rates of between 12 and 14 m/ka result in lagoonal characteristics closest to the observed data. The volume of re-deposited sand is fairly constant between those scenarios reaching sea level, however, the proportion of sand deposited in the lagoon versus behind the leeward margin varies (Fig. 7B–D).

Analysis of the modelled and observational data (Fig. 7E, F) shows that the greater the platform margin production rate, the earlier the sea level catch-up time for both the windward and leeward margins. However, the windward margin in the different scenarios never catches up with sea level as early as observed in the dated drill cores and the leeward only catches up 'on time' with production

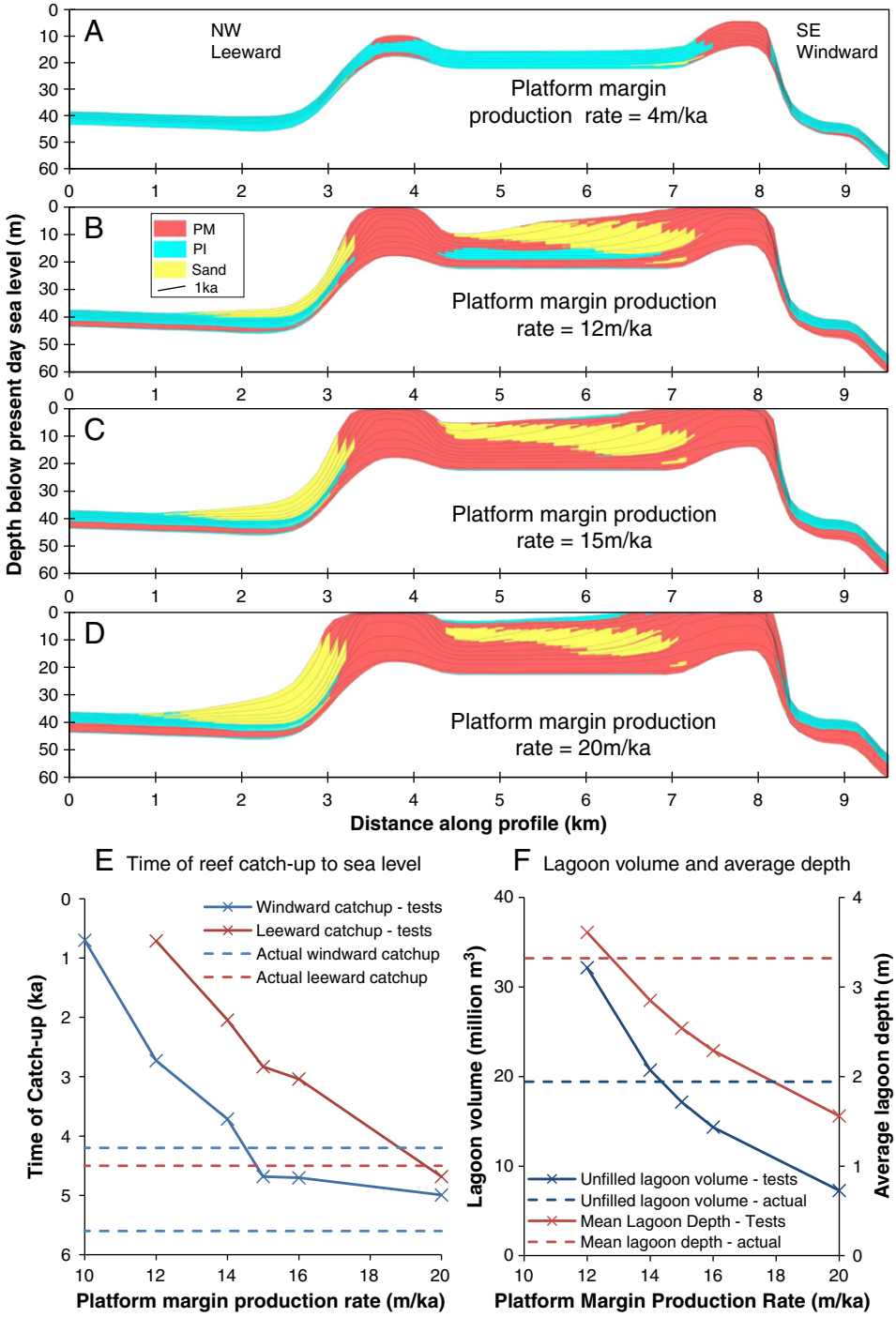

Fig. 7. Platform margin production rate model output test. A–D: Cross sections showing process-based sedimentary facies for different platform margin production scenarios. E: Plot showing relationship between platform margin production rate and timing of reef catch-up to sea level. F: Plot showing the relationship between platform margin production rate and lagoonal depth and volume.

rates of almost 20 m/ka. For the windward margin, increasing rates past 15 m/ka produces only a minor change in the time of sea level catch-up.

3.4. Sea level curve tests

The nature of sea level rise significantly influenced the morphology and internal facies patterns (Fig. 8) with the fastest the rate of rise (Fig. 8C, meltwater pulse) producing the deepest and most defined the "bucket" morphology. At these faster rates of sea level rise these distinct bucket shaped lagoons (as predicted by Schlager (2005)) form as the windward and leeward margins have sufficient accommodation space to grow faster than the restricted lagoonal area. However, a sea level rise of 45 m/ka during flooding was also tested but the output was nearly identical to the 25 m/ka scenario indicating some sort of upper sea level threshold was reached by the model. The sudden increase in water depth above the reef may reduce the realised accretion rate as the reef is no longer in the most productive upper few meters of the water column.

In the Caribbean style sea level rise scenarios, particularly the 0 k still stand (Fig. 8A), only the windward margin reaches sea level and little lagoonal sand is produced. In contrast to the rapid sea level rise case,

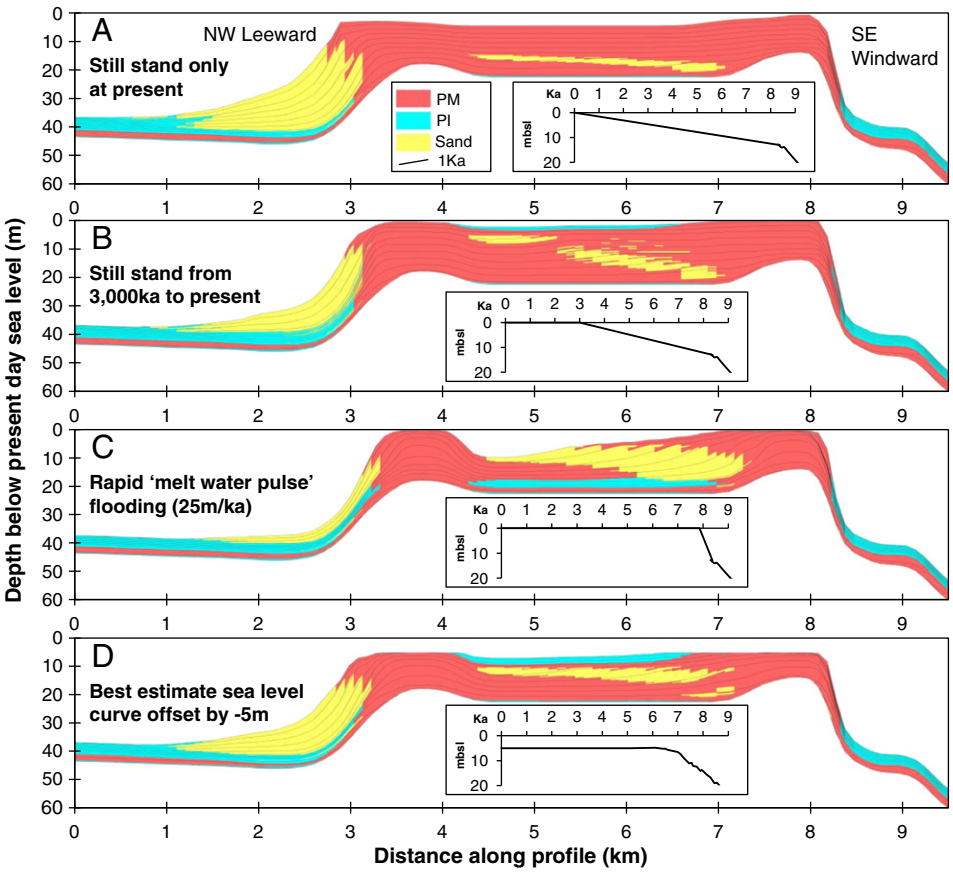

E

		Still stand starts 0Ka	Still stand starts 3,000Ka	Still stand starts 7,000Ka (Best estimate)	Rapid 'melt water pulse' flooding	Immediate flooding	Best estimate - 2m offset	Best estimate - 5m offset
	Lagoonal area (km^2)	No		7.26	8.70	9.30	6.32	4.86
	Mean lagoon depth (m)	Enclosed		2.85	3.66	4.37	4.00	6.14
	Unfilled lagoon volume (million m^3)	lagoon		20.72	31.84	40.69	25.34	29.84
Windward	Sea level catch-up (ka)	-	0.76	3.71	3.65	2.02	3.79	3.84
	Maximum vertical accretion (m/ky)	1.85	2.32	5.15	3.83	4.80	4.60	3.26
Leeward	Sea level catch-up (ka)	-	0.03	2.04	0.98	0.34	2.73	3.98
	Maximum vertical accretion (m/ky)	1.81	2.45	3.86	3.85	3.72	3.59	3.53
Lagoon	Maximum vertical accretion (m/ky)	3.42	3.84	4.27	4.59	3.36	4.25	3.90

Fig. 8. Sea level curve model output test. A–D: Cross sections showing process-based sedimentary facies for different sea level curve scenarios. E: Table of model output metrics for each sea level curve scenario.

this scenario recorded the largest leeward progradation of the leeward margin and sand wedge. Reef accretion lags several meters behind sea level and only catches right up during still stands (Fig. 8A, B) consistent with observations made by Marshall and Davies (1982) and referred to as a "Katch up 2" reef growth strategy (summarized by Davies, 2011). This lack of accommodation space represents a significant restricting factor on the potential accretion rate of the windward and leeward margins. This reduces the difference between lagoonal and margin accretion rates resulting in a flattening of the initial surface bucket morphology. Further reductions in accommodation space, simulated by a −5 m sea level, also produce a very small and shallow lagoon.

Given the models sensitivity to sea level changes, two additional curves were tested: (1) several oscillations of ~±1−2 m present day sea level (Lewis et al., 2008) and (2) a ~+1.5 m overshoot of present day sea level starting ~8 ka (Sloss et al., 2007). Despite only minor changes in the sea level curve, the repeated oscillations (Lewis curve) test produced a result similar to the best estimate with a slightly larger lagoonal depth/volume while the overshoot (Sloss curve) test resulted in a much deeper (>10 m) lagoon with less re-deposited sediment.

3.5. Disintegration rate tests

Simulations with no disintegration (Fig. 9A) produced a deep bucket morphology but with no re-deposited sand in either the lagoon or the leeward margin. Moderate rates of disintegration (0.05–0.07 m/ka) increase the amount of re-deposited sand in the model output leading to increased lagoonal filling (i.e., shallower lagoon)

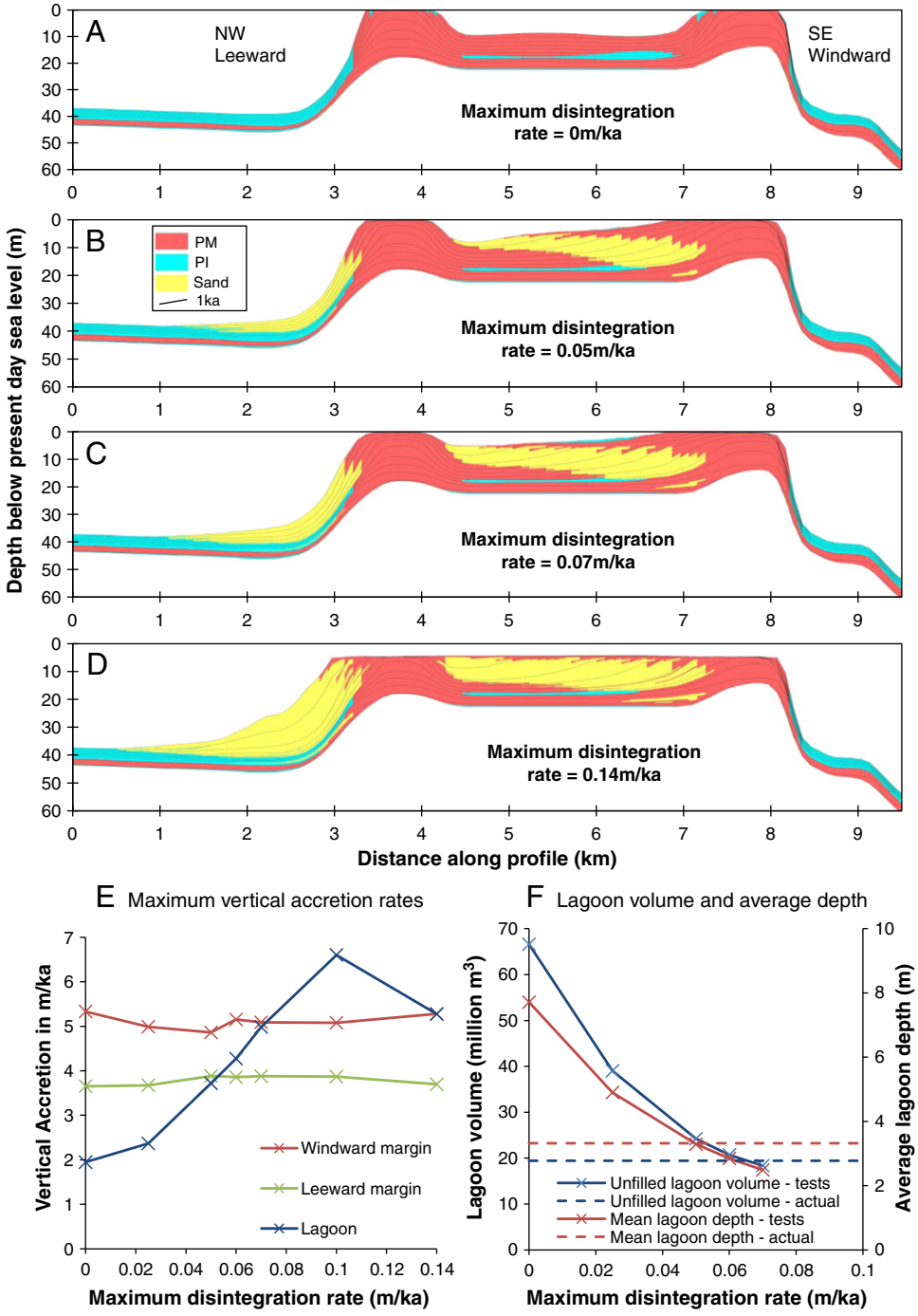

Fig. 9. Maximum disintegration rate model output test. A–D: Cross sections showing process-based sedimentary facies for different disintegration rate scenarios. E: Plot showing the relationship between disintegration rate and maximum vertical accretion at lagoon and windward and leeward margins. F: Plot showing relationship between disintegration rate and lagoon volume and average depth.

via progradation and a larger leeward sand wedge closest to the observed data. Disintegration rates as high as 0.14 m/ka (Fig. 9D) generated even larger volumes of re-deposited sand infilling lagoon and forms a large leeward sand wedge but these models stop accreting at about 4 m below sea level. These patterns are reflected in the relationships between the maximum vertical accretion rate on the margins and in the lagoon (Fig. 9E), with rates for both margins remaining constant at different disintegration rates. As expected, the rate of lagoonal accretion increases with increasing disintegration except at very high rates. Similarly, as the disintegration rate increases the level of lagoonal filling increases (i.e., decreasing volume and average depth) until no enclosed lagoon is formed due to the rims no longer reaching sea level.

The best estimate and range of disintegration values tested are significantly smaller some of the reported rates (see Section 2.2.5). These rates usually refer to only localised measurements and exposed reef rock rather than living organisms such as corals, and therefore may not be representative of the average disintegration over much larger areas of diverse substrates (i.e., across the reef) (Trudgill, 1983). Observed reductions in reef height may not directly relate to the volume of sediment available for transport as some sediment can be quickly incorporated within the reef framework via early

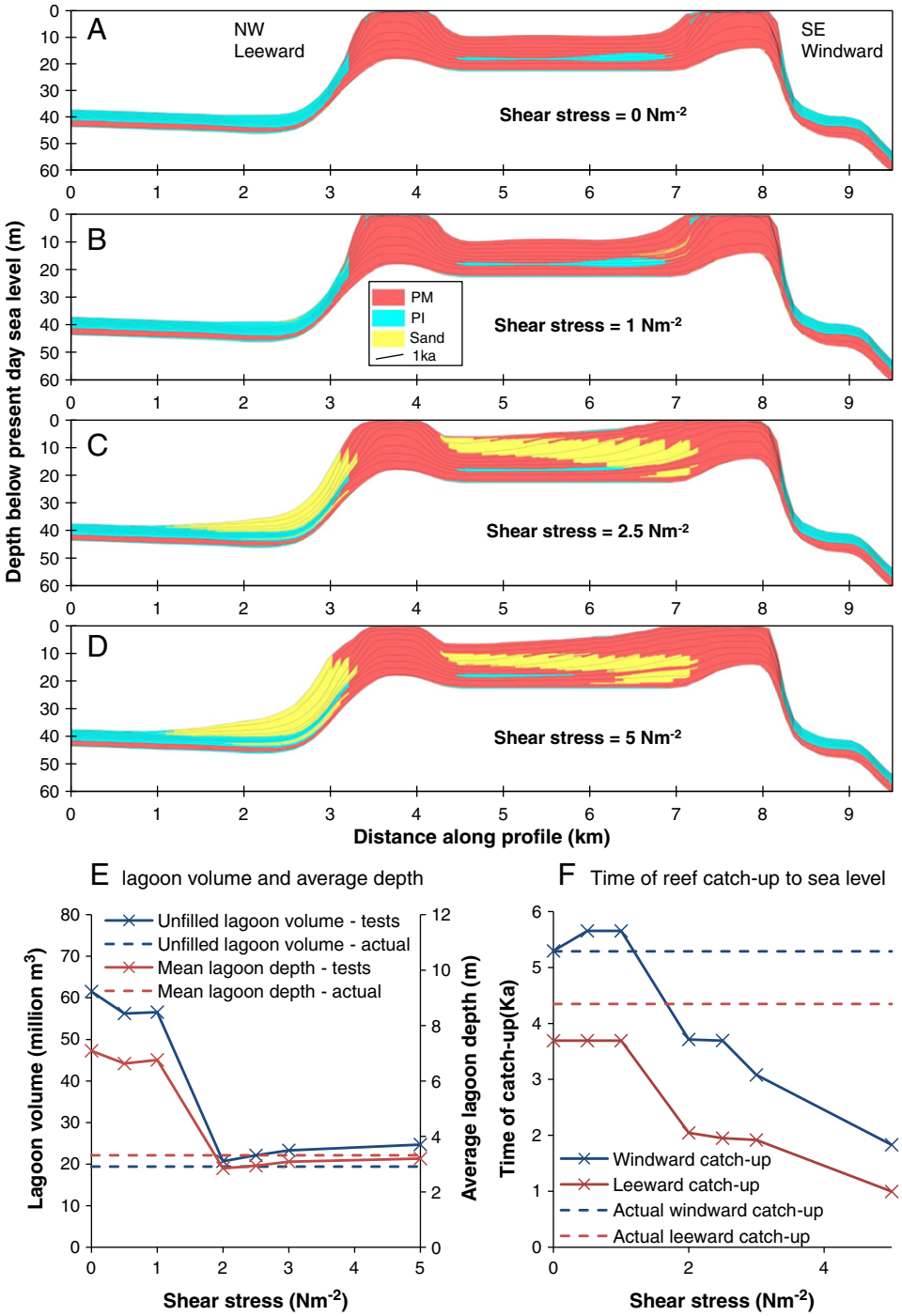

Fig. 10. Shear stress model output test. A–D: Cross sections showing process-based sedimentary facies for different shear stress scenarios. E: Plot showing the relationship between shear stress, lagoonal depth and volume. F: Plot showing relationship between shear stress and timing of reef catch-up to sea level.

lithification (cementation) and/or trapping and binding by coralgal and microbial accretion to become internal sediments (Seard et al., 2011).

3.6. Shear stress tests

Low shear stress values result in enhanced deep bucket morphologies free of re-deposited sand (Fig. 10A, B). Higher shear stress values (2.5–5 N m^2) increase the amount of sand which is transported to the leeward margin from the lagoon but result in lagoon morphologies and stratigraphies close to the best estimate model. These patterns are also confirmed in the analysis of the relationship between lagoonal volume and depth and the shear stress (Fig. 10E, F). Timing of both windward and leeward catch-up is later with increasing shear stress with values below 1 N m^{-2} resulting in modelled catch-up timing closest to those observed from the dated drill cores.

As erosion is the transport of disintegrated sediments, both disintegration and shear stress can also be considered together. Our modelling shows that either no shear stress (Fig. 10A) or no disintegration (Fig. 9A) also results in no sediment transport and deposition into the lagoon or leeward edge. In both cases this causes a deep, bucket morphology, free of re-deposited sediment, to form. Erosion and therefore both disintegration and shear stress are required to

Table 3
Reef maturity classification matrix of parameter testing model outputs colour coded by reef maturity stage.

Parameter	A	B	C	D	E	F
Initial surface	Deep initial flat-top (22 m–Fig 5D)	Deeper initial lagoon (13 m, 17 m, 26 m–Fig 5B)	Moderate depth initial flat-top (17 m)	No initial lagoon (13 m, 17 m, 17 m–Fig 5A)	Shallow initial flat-top (13 m–Fig 5C)	Very shallow initial flat-top (10 m)
Platform margin production	Extremely low (4 m/ka–Fig 7A)	Very low (10 m/ka)	Low (12 m/ka–Fig 7B)	High (15 m/ka–Fig 7C)	Very high (16 m/ka)	Extremely high (20 m/ka–Fig 7D)
Sea level curve	Very slow flooding (still stand at 0 ka–Fig 8A)	Slow flooding (still stand at 3 ka–Fig 8B)	Very fast flooding (25 m/ka sea level rise – Fig 8C)	Immediate flooding	2 m less accommodation space	5 m less accommodation space (Fig 8D)
Shear stress	None (0 Nm^{-2}–Fig 10A)	Very low (0.5 Nm^{-2})	Low (1 Nm^{-2}–Fig 10B)	High (2.5 Nm^{-2}–Fig 10C)	Very high (3 Nm^{-2})	Extreme (5 Nm^{-2}–Fig 10D)
Disintegration	None (0 m/ka–Fig 9A)	Very low (0.025 m/ka)	Low (0.05 m/ka–Fig 9B)	High (0.7 m/ka–Fig 9C)	Very high (0.1 m/ka)	Extreme (0.14 m/ka –Fig 9D)
Disintegration with high platform margin production	None (0 m/ka)	Very low (0.025 m/ka)	Low (0.05 m/ka)	Very high (0.1 m/ka)	Extreme (0.14 m/ka)	Extreme D. and PM Prod. (0.14 m/ka and 25 m/ka)

One tree reef stage timing	Sub–stage	Maturity stage	GBR examples
>5 ka ago	Submerged reef	Juvenile	–
~4–5 ka ago	Patch reef		17–065 (Central)
~2–3 ka ago	Crecentic	Mature	Britomart (Central)
–	Lagoonal (early filling)		One Tree / Fitzroy (Capricorn)
~2 ka ago to ~3 ka in the future[a]	Lagoonal (late filling)		
>~3 ka in the future[a]	Planar	Senile	Fairfax / Wreck (Capricorn)
	Submerged planar (special case)		

[a] based on time of platform interior domination of <2 m deep lagoon – see section 4.1

form the partially filled bucket morphology observed at One Tree Reef and are important factors controlling reef maturity.

4. Discussion

We find that our best estimate model simulated the Holocene evolution of One Tree Reef with impressive accuracy when compared to the observed data. More importantly, our sensitivity experiments allowed us to assess the impact of the different factors or parameters on reef development. Below we: (1) discuss the best estimate model and how and why the model deviates from the observational data; (2) evaluate the importance of the main parameters in controlling reef evolution and; (3) discuss the implications and limitations of this numerical model-observational approach for providing insights into long standing ideas about reef evolution and maturity.

4.1. Towards a 3D model of Holocene reef evolution

Qualitative visual comparison between the best estimate model outputs (Fig. 4) and the observational data (e.g., Marshall and Davies, 1982) (Fig. 2) show considerable similarities in reef morphology, stratigraphy, surface and subsurface facies patterns. The model lagoonal area, depth and volume are similar (within 25%, Fig. 4D) to the observed morpho-metric data. The higher modelled lagoon area (124% of the observed) and low depth (86% of the observed) balance out forming a lagoon only 7% greater than the actual lagoon volume (Fig. 4D). The gently sloping and deepening of the lagoon floor leewards observed in both the model and the bathymetric data (Fig. 2B) suggests the sediment depositional patterns in the lagoon (mainly leeward progradation) are being reasonably simulated. However, the model does not simulate the well-developed sub-tidal

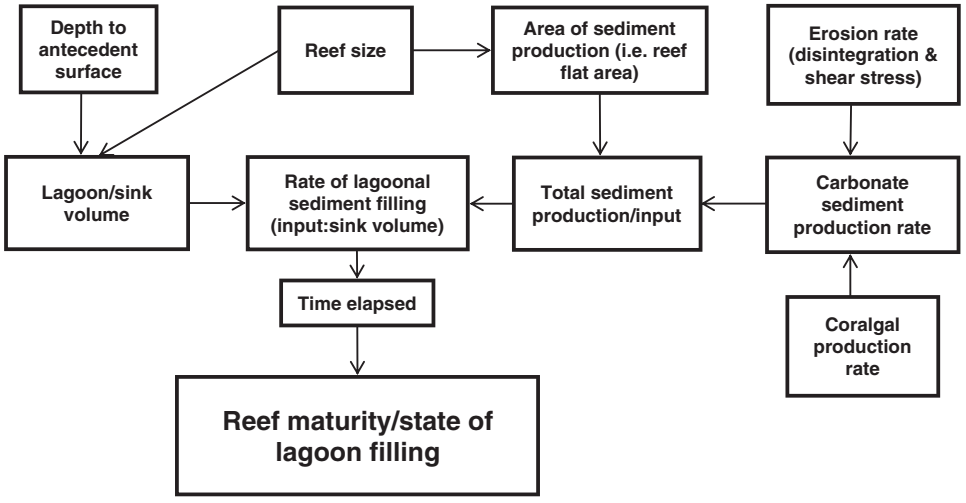

Fig. 11. Conceptual model illustrating the relationships between reef maturity and the main controlling factors.

sandsheet observed leeward of the southern and eastern reef flats at One Tree (Fig. 2A, B) and many other reefs in the GBR (Hopley et al., 2007) and elsewhere (e.g., Belize; Purdy and Gischler, 2005). This may be due to the lack of a more detailed hydrodynamic model for sediment transport within CARB3D. In the model, shear stress is applied equally across the whole model area and therefore, sand cannot be deposited above the depth which represents the transition between sand entrainment and sand deposition. This boundary is clearly visible in Fig. 4A where re-deposited sand does not appear shallower than 6 m at any point in the lagoon or the leeward margin.

The modelled reef's internal stratigraphic and chronologic structure is complex and heterogeneous throughout (Fig. 5), as is predicted and observed by Marshall and Davies 1982. The actual sedimentary facies are not modeled in CARB3D (i.e., coral heads, branching coral etc.), however, the simulated defined facies are similar (Fig. 4B). Here framestones dominate the margins with the lagoon sands (grainstones and packstones) along with significant coralgal framework in the form of platform margin production in 'boundstones'. The distribution of these facies is broadly consistent with conceptual facies models for One Tree (Fig. 2C) and other Indo-Pacific Holocene reefs (Montaggioni, 2005). However, some patterns such as large amounts of in situ coralgal material in the lagoon are less so. While sediments in the modern One Tree lagoon are mainly sand and mud (Davies, 1983), a significant proportion of lagoonal area (~30%) is characterised by in situ coralgal material forming patch reefs (Fig. 2A). While CARB3D cannot directly simulate small patch reefs, the proportion of the modern lagoon comprising patch reefs versus sediments is similar the general model output of boundstone with ~30–60% coralgal material.

The observed vertical accretion and sea level catch-up timing vary significantly between drill holes (Marshall and Davies, 1982) (Fig. 4C). Despite this natural variability, the modelled accretion curves do show a similar shape to the observational data. However, at some locations, the actual reef reached sea level significantly before the modelled reef, while in other areas, the opposite is true. While final morphology and basic stratigraphic patterns may be similar, closer examination of the modelled reef evolution indicates several important points of difference. It appears that while the modelled accretion rates fall within the range of observed values (Davies and Hopley, 1983), the rates of vertical accretion that dominate the sea level catch-up period are too low while the lateral progradation rates during the still stand are too high, resulting in the modelled reef margins being wider than the observed. Combined with problems simulating sand transport and deposition, the model by itself will not directly predict the precise timing or structure of the final stage of lagoonal filling to sea level which Davies (1983) predicted would take about 5 ka. However, if we consider when the platform interior production dominates the shallow lagoon (~<2 m) then this stage could reasonably classified as "filled" planar reefs and thus a model analogue for a senile reef. Therefore, in this context it is possible to use our model outputs (Figs. 4–10) to quantitatively establish which parameters, and more importantly what rates, are important in controlling reef evolution and maturity across a range reef types and settings in the GBR and other regions (e.g., Table 3).

4.2. Implications for coral reef maturity

The full range reef maturity classification (i.e., juvenile to senile/planar) is represented in the model outputs (Table 3). We also included a special classification of submerged planar reefs where reefs reached apparent full maturity at the wave base rather than the sea surface. We find that accommodation space (i.e., the initial surface) and the way in which this space is modified (i.e., sea level rise and vertical growth) exert strong controls on maturity; scenarios defined by lower accommodation space generally being more mature. Shear stress and disintegration, together representing erosion, affect the transition between lagoonal and planar reefs, but not earlier juvenile stages. The platform margin production rate also strongly controls the maturity across the full range from juvenile to senile/planar. The best estimate model transitions through time from juvenile to senile/planar (when run beyond the present day) but only encloses a lagoon once the lagoon is partially filled, thereby skipping the early lagoonal filling stage.

Hopley et al. (2007; Hopley, 2011) suggested the main factors controlling present reef maturity are: (1) the depth to the antecedent surface (or alternatively, the total Holocene accommodation space); (2) the size of the reef (specifically the ratio of reef rim area to lagoonal area) or potentially; (3) variations in production rates. Our modelling confirms that the antecedent surface/accommodation space is perhaps the important controlling factor. As noted by previous workers, accommodation space affects the volume of the reef lagoon, and therefore the potential sediment sink volume (e.g., Davies, 1983). The nature of sea level rise also has a significant impact on maturity outputs. However, Holocene sea level rise (Lambeck and Chappell, 2001) in the Capricorn-Bunker region (Sloss et al., 2007) with its range of observed reef maturity types, is unlikely to have varied significantly. Relative sea level curves may be an important factor determining reef maturity but in regions where uplift (e.g., Lambeck and Chappell, 2001), subsidence (e.g., Webster et al., 2009) or glacial-hydro-isostatic considerations (Nakada and Lambeck, 1989) vary significantly in space and time.

Our platform margin production simulations agree with previous ideas (Davies, 2011; Hopley, 2011) about the impact of different rates on reef maturity. Sediment production based on coralgal framework (platform margin) production rates along with erosion (disintegration and shear stress) controls both whether the reef reaches sea level in the modelled time period, and the amount of sediment filling in the lagoon. While coralgal carbonate production and erosion may vary significantly at the local reef scale, in general these rates are unlikely to vary enough between reefs to explain the range of reef maturities observed in the Central and Southern GBR (Table 3). The special case of planar reefs forming at the wave base rather than at sea level under very high erosion conditions occurs where erosion overtakes all sediment production in the upper part of the water column, preventing the reef from reaching sea level. This reef form is not observed in the GBR.

The controls on reef maturity summarized by Hopley (2011) and Davies (2011), and tested quantitatively by our modelling, indicate that relative proportion of sediment generation and size of the sediment sink (i.e., the lagoon) is also fundamentally important. This can be simply conceptualised in the context of factors that broadly control sediment generation and the size of the sediment sink (Fig. 11). For example, the amount of sediment produced at the reef flat is influenced by size/area of the reef flat, the rates of disintegration and transport into the sink, the replacement of eroded material (i.e., reef re-growth) and the factors which affect each of these in turn. This conceptual model of reef maturity controls may be expanded in future to include other major and minor controlling factors. For example, such a model could be used to predict wide scale erosion rates where the other variables are well known.

Using this conceptual model, it might also be possible to create a predictive 3D numerical model of future reef trajectories based on known factors (e.g., substrate depth and reef size). This could be tested using the range of observed reef maturity types in Capricorn-Bunker group (Table 3) where factors such as the depth to the antecedent surface and growth histories are known for several Holocene reefs (Davies and Hopley, 1983). For example, running our best estimate model forward in time indicates that for One Tree Reef, currently a mature reef, becomes a senile reef (although not fully filled by sand) after about 3 ka in contrast to Davies' (1983) qualitative prediction of 5 ka.

4.3. 3D numerical modelling strengths, weakness and future directions

CARB3D simulated the Holocene evolution of One Tree Reef with impressive accuracy, matching >75% for the key morphometrics,

while sensitivity testing allowed us to assess the relative importance of different controlling factors on reef morphology, accretion and facies patterns and maturity. We argue that this approach could also be successfully applied to other reefs in the GBR and other regions that are less studied than One Tree Reef. However, in the process we identified several important limitations in our application of CARB3D to modelling Holocene reefs. First, the models limitations in simulating small spatial and temporal scales meant that some important reef features (e.g., sub-tidal sandsheet, lagoonal patch reefs) could not be represented. Second, biological patterns of coralgal growth (spawning, recruitment, environmental thresholds, time lags etc.) are highly complex, can vary significantly locally (Davies 1983; Montaggioni 2005; Abbey et al., 2011), and are difficult to simulate numerically. One example relates to coral larvae in the real world preferentially colonising hard surfaces (e.g., exposed reef rock) rather than soft and mobile sediments (e.g., sand or mud). This results in patch reefs and reef margins primarily growing vertically rather than laterally (unless restricted by sea level) forming the steep sided accumulations. CARB3D does not simulate these processes—coralgal production is not dependent on substrate—which led to more lateral coralgal progradation and wider reef rims in the model outputs. Another biological consideration not simulated is the still controversial time lag (Davies and Hopley, 1983; Hopley, 2011) due to inimical conditions that follows the initial flooding of the basement substrate and then reef turn-on. Third, and perhaps most challenging, is the simplified hydrodynamic models incorporating disintegration and shear stress. CARB3D does not allow features like the sand sheet to form and the specific lack of wave refraction and tidal currents does not allow for realistic local sediment transport and movement. For example, the coarse coral rubble deposits that form the island itself and the eastern flat could not be simulated (Fig. 2). High-energy, low frequency storm processes responsible for these deposits are poorly understood (Gourlay 1988; Thornborough and Davies 2011) and even less so in the context of numerical modelling. Better constraints on the physical processes (Kench and Brander, 2006; Harris et al. 2011) involved in sediment generation, transport and deposition will allow more realistic computer models with higher spatial and temporal resolution to investigate the response of coral reef systems to the effects of global climate change past and future (e.g., Salles et al. 2011; Storlazzi et al. 2011).

5. Conclusions

Based on a synthesis of available field observations and 3D numeral modelling data from One Tree Reef in the southern GBR, we draw the following conclusions:

1. CARB3D and the input parameters can be used to successfully model Holocene reef evolution in the GBR. Quantitative comparisons between our “best estimate” model output and the observed data confirm that we are able to simulate a greater than 75% match for the main morphologic and growth characteristics of One Tree Reef. This approach could therefore be applied to other Holocene reefs in the GBR and elsewhere.
2. Sensitivity testing produced the known range of reef maturity morphologies (juvenile to senile). We quantitatively demonstrate that depth and shape of the antecedent topography is a major control on the state of reef maturity in the GBR. However, the commonly “bucket” shaped Holocene reef morphology can also result from preferential reef margin growth alone, or act to amplify the initial surface topography. Other simulations show that sea level, sediment erosion and transport can also exert a strong control on reef morphology and maturity, by controlling lagoon filling.
3. Modelling indicates that the Holocene reef is characterised by complex internal structures and stratigraphies, including significant 3D variations in sedimentary facies patterns and chronologies. In this sense, our modelling approach could be used to make realistic predictions for other GBR reefs and elsewhere in settings where drill core coverage maybe sparse.
4. The model was unable to generate finer scale geomorphic structures (e.g., sub-tidal sand sheets and patch reefs). Limitations in CARB3D's hydrodynamic model, combined with a lack of realistic reef “turn-on” lag and coralgal spawn/recruitment patterns prevented the simulation of these fine-scale geomorphic features. To better reconstruct the past development of GBR, as well as make accurate assessments of possible future trajectories of reefs in general, new models must incorporate more realistic representations of hydrodynamic, biologic and sedimentary processes that operate on finer temporal and spatial scales.

Supplementary materials related to this article can be found online at doi:10.1016/j.sedgeo.2012.03.015.

Acknowledgments

We thank the Australian Hydrographic Service for the permission to use the LADS data and Robin Beaman at James Cook University for the data processing of some of the bathymetry data sets. We are grateful to Georg Warrlich for his assistance using CARB3D, Elizabeth Abbey for help with the figures and Alisha Thompson for an earlier review of the manuscript. The study was supported by the University of Sydney Start-Up funding to JMW. We also thank Brian Jones and an anonymous reviewer for their constructive reviews of this manuscript.

References

Abbey, E., Webster, J.M., Braga, J.C., Sugihara, K., Wallace, C., Iryu, Y., Potts, D., Done, T., Camoin, G., Seard, C., 2011. Variation in deglacial coralgal assemblages and their paleoenvironmental significance: IODP Expedition 310, "Tahiti Sea Level". Global and Planetary Change 76, 1–15.
Bard, E., Hamelin, B., Fairbanks, R.G., 1990. U–Th ages obtained by mass spectrometry in corals from Barbados: sea level during the past 130,000 years. Nature 346, 456–458.
Davies, P.J., 1977. Modern reef growth—Great Barrier Reef. Proceedings of the Second International Coral Reef Symposium 2, 326–330.
Davies, P.J., 1983. Reef growth. In: Barnes, D. (Ed.), Perspectives on Coral Reefs. Brian Clouston Publisher, Manuka, ACT: AIMS.
Davies, P.J., 2011. Great Barrier Reef: origin, evolution and modern development. In: Hopley, D. (Ed.), Encyclopedia of Modern Coral Reefs: Structure, Form and Process. Springer, pp. 504–534.
Davies, P.J., Hopley, D., 1983. Growth fabrics and growth rates of Holocene reefs in the Great Barrier Reef. BMR Journal of Australia Geology and Geophysics 8, 237–251.
Davies, P.J., Kinesy, D.W., 1977. Holocene reef growth—One Tree, Great Barrier. Marine Geology 24, M1–M11.
Davies, P.J., Montaggioni, L., 1985. Reef growth and sea level change: the environmental signature. Proceedings of the Fifth International Coral Reef Symposium, Taihiti, pp. 477–515.
Davies, P.J., Radke, B.M., Robinson, C.R., 1976. The evolution of One Tree Reef, Southern Great Barrier Reef, Queensland. BRM Journal of Australian Geology & Geophysics 1, 231–240.
Davies, P.J., Thom, B.B., Short, A., Marshall, J.F., Harvey, N., Martin, K., 1977. Reef development—Great Barrier Reef. Proceedings of the Third International Coral Reef Symposium, Miami, 2, pp. 331–337.
Davies, P.J., Symonds, P.A., Feary, D.A., Pigram, C.J., 1988. Facies models in exploration—the carbonate platforms of north-east Australia. The APEA Journal 28, 123–143.
Davies, P.J., Symonds, P.A., Feary, D.A., Pigram, C.J., 1989. The evolution of the carbonate platforms of northeast Australia, controls on carbonate platform and basin development. Society of Economic Paleontologists and Mineralogists 233–258.
Dunham, R.J., 1962. Classification of carbonate rocks according to depositional texture. In: Ham, W.E. (Ed.), Classification of carbonate rocks: American Association of Petroleum Geologists Memoir, pp. 108–121.
Embry, A.F., Klovan, J.E., 1971. A Late Devonian reef tract on Northeastern Banks Island, NWT. Canadian Petroleum Geology Bulletin 19, 730–781.
Fairbanks, R.G., 1989. A 17,000-year glacio-eustatic sea level record: influence of glacial melting rates on the Younger Dryas event and deep-ocean circulation. Nature 342, 637–642.
Frith, C.A., Mason, L.B., 1986. Modelling wind driven circulation One Tree Reef, Southern Great Barrier Reef. Coral Reefs 4, 201–211.
Gourlay, M.R., 1988. Coral cays: products of wave action and geological processes in a biogenic environment. Proceedings of the 6th International Coral Reef Symposium, Townsville, Australia, 2, pp. 491–496.

Harris, D.L., Webster, J.M., De Carli, E.V., Vila-Concejo, A., 2011. Geomorphology and morphodynamics of a sand apron, One Tree Reef, Southern Great Barrier Reef. Journal of Coastal Research SI (64), 760–764.
Harvey, N., Hopley, D., 1981. The relationship between modern reef morphology and a pre-Holocene substrate in the Great Barrier Reef Province. Proceedings of the Fourth International Coral Reef Symposium, Manila 1, 549–554.
Harvey, N., Davies, P.J., Marshall, J.F., 1979. Seismic refraction—a tool for studying coral reef growth. BRM Journal of Australian Geology & Geophysics 4, 141–147.
Hopley, D., 1982. The Geomorphology of the Great Barrier Reef: quaternary development of coral reefs. Wiley, New York.
Hopley, D., 2011. Reef Classification by Hopley (1982). In: Hopley, D. (Ed.), Encyclopedia of Modern Coral Reefs: Structure. Springer, Form and Process, pp. 850–854.
Hopley, D., Smithers, S.G., Parnell, K.E., 2007. The geomorphology of the Great Barrier Reef. Cambridge.
Hubbard, D.K., Miller, A.I., Scaturo, D., 1990. Production and cycling of calcium carbonate in a shelf-edge reef system (St. Croix, U.S. Virgin Islands); applications to the nature of reef systems in the fossil record. Journal of Sedimentary Research 60, 335–360.
Kench, P.S., Brander, R.W., 2006. Wave processes on coral reef flats: implications for reef geomorphology using Australian case studies. Journal of Coastal Research 22, 209–223.
Lambeck, K., Chappell, J., 2001. Sea level change through the last glacial cycle. Science 292, 679–686.
Lewis, S.E., Wust, R.A.J., Webster, J.M., Shields, G.A., 2008. Mid-late Holocene sea-level variability in eastern Australia. Terra Nova 20, 74–81.
Marshall, J., Davies, P.J., 1982. Internal structure and Holocene evolution of One Tree Reef, Southern Great Barrier Reef. Coral Reefs 1, 21–28.
Marshall, J.F., Davies, P.J., 1984. Last interglacial reef growth beneath modern reefs in the southern Great Barrier Reef. Nature 307, 44–47.
Montaggioni, L.F., 2005. History of Indo-Pacific coral reef systems since the last glaciation: development patterns and controlling factors. Earth-Science Reviews 71, 1–75.
Montaggioni, L.F., Braithwaite, C.J.R., 2009. Quaternary coral reef systems: history, development processes and controlling factors. Developments in Marine Geology. Elsevier.
Nakada, M., Lambeck, K., 1989. Late Pleistocene and Holocene sea-level change in the Australian region and mantle rheology. Geophysical Journal International 96, 497.
Purdy, E.G., Gischler, E., 2005. The transient nature of the empty bucket model of reef sedimentation. Sedimentary Geology 175, 35.
Salles, T.B., Griffiths, C.M., Dyt, C.P., Li, F., 2011. Australian shelf sediment transport responses to climate change-driven ocean perturbations. Marine Geology 282, 268–274.
Schlager, W., 2005. Carbonate Sedimentology and Sequence Stratigraphy. SEPM, Tulsa, USA.
Seard, C., Camoin, G., Yokoyama, Y., Matsuzaki, H., Durand, N., Bard, E., Sepulcre, S., Deschamps, P., 2011. Microbialite development patterns in the last deglacial reefs from Tahiti (French Polynesia; IODP Expedition #310): implications on reef framework architecture. Marine Geology 279, 63–86.
Searle, D.E., Harvey, N., Hopley, D., Johnson, D.P., 1982. Significance of results of shallow seismic research in the Great Barrier Reef Province between 16° 10'S and 20° 05'S. Proceedings of the Fourth International Coral Reef Symposium, Manila.
Sloss, C.R., Murray-Wallace, C.V., Jones, B.G., 2007. Holocene sea-level change on the southeast coast of Australia: a review. The Holocene 17, 999–1014.
Smith, B.T., Frankel, E., Jell, J.S., 1998. Lagoonal sedimentation and reef development on Heron Reef, southern Great Barrier Reef Province. Special Publications of the International Association of Sedimentologists 25, 281–294.
Spencer, T., 1985. Marine erosion rates and coastal morphology of reefal limestones on Grand Cayman Islands, West Indies. Coral Reefs 4, 59–70.
Stoddart, D.R., 1973. Coral reefs of the Indian Ocean. In: Jones, O.A., Endean, R. (Eds.), Biology and geology of coral reefs. Academic Press, London, pp. 51–92.
Storlazzi, C.D., Elias, E., Field, M.E., Presto, M.K., 2011. Numerical modeling of the impact of sea-level rise on fringing coral reef hydrodynamics and sediment transport. Coral Reefs 30, 83–96.
Stuiver, M., Reimer, P.J., Bard, E., Warren Beck, J., Burr, G.S., Hughen, K.A., Kromer, B., McCormac, G., Van Der Plicht, J., Spurk, M., 1988. INTCAL98 radiocarbon age calibration, 24,000–0 cal BP. Radiocarbon 40, 1041–1083.
Thornborough, K.J., Davies, P.J., 2011. Reef Flats. In: Hopley, D. (Ed.), Encyclopedia of Modern Coral Reefs: Structure, Form and Process. Springer, pp. 869–875.
Toscano, M.A., Peltier, W.R., Drummond, R., 2011. ICE-5G and ICE-6G models of postglacial relative sea-level history applied to the Holocene coral reef record of northeastern St Croix, U.S.V.I.: investigating the influence of rotational feedback on GIA processes at tropical latitudes. Quaternary Science Reviews 30, 3032–3042.
Trudgill, S.T., 1983. Preliminary estimates of intertidal limestone erosion, One Tree Island, Southern Great Barrier Reef, Australia. Earth Surface Processes and Landforms 8, 189–193.
Vecsei, A., 2001. Fore-reef carbonate production: development of a regional census-based method and first estimates. Palaeogeography, Palaeoclimatology, Palaeoecology 175, 185–200.
Warrlich, G.M.D., Waltham, D.A., Bosence, D.W.J., 2002. Quantifying the sequence stratigraphy and drowning mechanisms of atolls using a new 3-D forward modelling program (CARBONATE 3D). Basin Research 14, 379–400.
Warrlich, G., Bosence, D., Waltham, D., Wood, C., Boylan, A., Badenas, B., 2008. 3D stratigraphic forward modelling for analysis and prediction of carbonate platform stratigraphies in exploration and production. Marine and Petroleum Geology 25, 35–58.
Webster, M.A., Petkovic, P., 2005. Australian Bathymetry and Topography—digital dataset. Record 2005/12. In: Geoscience Australia (Ed.), . Canberra, Australia.
Webster, J.M., Wallace, L., Clague, D., Braga, J.C., 2007. Numerical modeling of the growth and drowning of Hawaiian coral reefs during the last two glacial cycles (0–250 kyr). Geochemistry Geophysics Geosystems 8. doi:10.1029/2006GC001415.
Webster, J.M., Braga, J.C., Clague, D.A., Gallup, C., Hein, J.R., Potts, D.C., Renema, W., Riding, R., Riker-Coleman, K., Silver, E., Wallace, L.M., 2009. Coral reef evolution on rapidly subsiding margins. Global and Planetary Change 66, 129–148.